Few Layer Graphene sticking by biofilm of freshwater diatom Nitzschia palea as a mitigation to its ecotoxicity

Marion Garacci, Maialen Barret, Florence Mouchet, Cyril Sarrieu, Pierre Lonchambon, Emmanuel Flahaut, Laury Gauthier, Jérôme Silvestre, Eric Pinelli

Few Layer Graphene sticking by biofilm of freshwater diatom *Nitzschia palea* as a mitigation to its ecotoxicity

M. Garacci [a], M. Barret [a], F. Mouchet [a], C. Sarrieu [b], P. Lonchambon [b], E. Flahaut [b], L. Gauthier [a], J. Silvestre [a], E. Pinelli [a, *]

[a] *EcoLab (Laboratoire d'Ecologie Fonctionnelle), Université de Toulouse, CNRS, INPT, UPS, Toulouse, France*
[b] *CIRIMAT, Université de Toulouse, CNRS, INPT, UPS, UMR, CNRS-UPS-INP No 5085, Université Toulouse 3 Paul Sabatier, Bât., CIRIMAT, 118, route de Narbonne, 31062 Toulouse Cedex 9, France*

A B S T R A C T

Carbon-based nanoparticles such as graphene have many applications leading to their industrial production. Few-Layer Graphene (FLG) is thus likely to be found in the environment, and especially in rivers. In this study, the effect of FLG on the photosynthetic benthic diatom *Nitzschia palea* was assessed making distinction between the impact of a direct contact with FLG and a shading effect of FLG on diatoms. Growth inhibition of diatoms exposed to FLG at 50 mg L^{-1} was observed at 48 h of exposure associated with an increase in diatoms mortality. At 144 h, the growth rate was recovered. However, in shading condition, at 48 h of FLG exposure, a persistent growth inhibition was observed at 50 mg L^{-1}. Microscopic observations and a monitoring of FLG concentration in the medium allowed to conclude that exopolymeric substances (EPS), naturally secreted by *N. palea*, strongly interact with FLG, sticking nanoparticles at the bottom of wells. Our results highlight the potential mechanisms of clarification of the water column by diatoms biofilms, by sticking FLG even at high concentration. Overall, these results suggest that one potential toxicity process of graphene could be a combination of direct and shading effect leading to a strong interaction between biofilm and nanoparticles.

1. Introduction

Nanotechnology is no more an emerging science and arouses more interest for few years. The interest for new nanomaterials is continuously growing [1], sustained by very intensive research work in this field [2,3]. Among the studied manufactured nanoparticles, graphene nanomaterial family (graphene and related materials), including Few Layer Graphene (FLG), is increasingly studied for its promising applications. FLG is a planar carbon-based particle which differs from bulk graphite by its nanometric thickness. This is the assembly of several monoatomic layers of carbon (graphene). Carbon atoms in each graphene sheet are bounded by sp^2 covalent bonds in a honeycomb lattice. The nanometric thickness of this material confers numerous interesting properties such as mechanical, electrical, thermal and optical properties [4–6], which open new prospects and emerging applications in several sectors ranging from energy [7,8] to the biomedicine [9,10].

Nevertheless, interaction of such particles with biological systems is in return difficult to predict and thus the emergence of FLG presents numerous environmental risks [11]. There is in fact a strong lack of information about effective quantities of carbon-based nanoparticles in circulation [1] and especially for graphene. FLG could be found in the environment at several steps of its life cycle and especially in aquatic ecosystems where most pollutants can be concentrated. The size of nanoparticles implies a great specific surface area, which plays an important role in the impact on organisms [12,13]. Although many studies on the toxicology of nanoparticles have been carried out *in vivo* to date on model organisms such as rat but also *in vitro* on human cells [14,15], studies aimed to investigate the effect of graphene in the Environment are scarce.

Most of ecotoxicological studies were carried out on the effect of functionalized graphene such as graphene oxide. Several toxicological studies reported the impact of graphene oxide on plants [16] and bacteria discussing its antibacterial properties. A cytotoxic effect of these nanoparticles on *Escherichia coli* or *Staphylococcus aureus* was evidenced [17]. Hu et al. [18] reported a strong

* Corresponding author.
E-mail address: pinelli@ensat.fr (E. Pinelli).

http://dx.doi.org/10.1016/j.carbon.2016.11.033

inhibition of *E. coli* (DH5α) growth in presence of 85 mg L^{-1} of graphene oxide. However, few years later, Ruiz et al. [19] observed an opposite effect with an increase in *E. coli* (JM109) proliferation exposed to the same range of concentration of graphene oxide. According to the authors, this growth activation might have been due to the use of graphene oxide as a growth scaffold, helped by an overproduction of EPS which could depend on the bacteria species. Nevertheless, only few studies have investigated the impact of FLG on organisms. Pretti et al. [20] investigated the impact of graphene mono layer flakes on several marine organisms and reported an inhibition of bioluminescence on the bioluminescent bacterium *Vibrio fischeri* with an EC_{50} value of 2 mg L^{-1}, but no effect on the crustacean *Artemia salina*. Several studies on *Daphnia magna*, a freshwater planktonic crustacean, demonstrated an accumulation of ^{14}C-labeled graphene in gut's organisms [21,22]. Another study revealed no toxic effect of multi-functional graphene on zebra fish embryos even at 100 mg L^{-1} [23].

Despite the low number of studies on algae, their crucial position in the aquatic food chain as primary producer and their important function in the carbon cycle [24] make them of particular interest for the assessment of contaminants effects [25]. Nevertheless, only a small fraction of the studies on graphene ecotoxicity was carried out on algae. A study on the green algae *Raphidocelis subcapitata* reported a shading effect caused by graphene oxide which contribute to reduce algal density [26]. Pretti et al. [20] showed that graphene mono layer flakes induced a growth inhibition on the unicellular algae *Dunaliella tertiolecta* from 1.25 mg L^{-1} of graphene. All studies carried out on graphene have shown a dose-dependent effect of this nanomaterial on biological systems without clear conclusion on the effects associated with shading or any direct toxicity [27].

The toxicity of nanomaterials on biological systems in the aquatic environment could be impacted by the presence of natural organic matter in the media. Thus, several recent studies aimed to understand fate and effects of graphene-based materials in the aquatic environment [28,29]. Wang et al. (2016) [29] demonstrated that the presence of organic acids improved the stability of graphene nanoplatelets suspension but had also an impact on the toxicity of nanoparticles on a unicellular green algae *Scenedesmus obliquus*. These authors observed a hormesis effect of low organic acids [29], implying the mitigating of graphene toxicity only at low concentration of organic acids resulting in a decrease of growth inhibition and oxidative stress on *Scenedesmus obliquus*.

Among algae, diatoms play a major role in the global primary productivity responsible at least of a quarter of the inorganic carbon fixed each year in the ocean [30]. Diatoms represent the main component of many photosynthetic biofilms during autumn and spring in freshwater [31]. These microalgae have the particularity to produce a cell wall, called frustule, composed of silica structure with different ornamentations. A particular feature of diatoms is their capacity to produce extracellular polymeric substances (EPS) mainly composed of polysaccharides and proteins [32]. The biofilm built with these EPS helps diatoms to adhere and grow on a substrate [33,34]. EPS can also have a role in the protection against pollutants such as metals thanks to an accumulation of metals in the polysaccharide matrix of the biofilm [35].

A recent study demonstrated original effects of carbon nanotubes (CNTs) on *Nitzschia palea* algae [36]. This study reported that CNTs caused a temporary growth inhibition linked to a shading effect without neither toxicity nor photosynthetic disruption. Furthermore, the authors highlighted the major role of EPS produced during the interaction between diatoms and nanoparticles.

In this study, the toxicity of FLG on the diatom *N. palea* (Kützing) W. Smith (*N. palea*) was assessed. The aim of this work was to determine the toxicity level of FLG on diatoms cells by studying three different endpoints such as growth inhibition, photosynthetic yield and cell viability. An original device previously developed by Verneuil et al. [36] was used. This device allows distinguishing the shading effect and the total effect (including direct contact and shading) of FLG on these benthic organisms. In addition, the interaction between the algal biofilm and FLG suspension has been investigated using complementary microscopic approaches.

2. Materials and methods

2.1. Diatom strain cultivation and graphene preparation

2.1.1. Diatom strain cultivation prior to exposure experiments

The axenic strain of *N. palea* CPCC-160 was provided by the Canadian Phycological Culture Center (University of Waterloo, Waterloo, ON, Canada). Algal cultures were grown under axenic conditions in a modified CHU no. 10 basic medium, called SPE medium (SPE; 6.4 < pH < 6.6) (Supplementary Table S1 for the detailed composition). Bioassays were carried out in a growth room at 22 ± 1 °C on a rotary shaker at 90 rpm with a light/dark period of 14 h/10 h supplied by high pressure sodium lamps (VIALOX® NAV® (SON) SUPER 4Y®, 400 W, OSRAM GmbH) at 120 μE. SPE medium was replaced by fresh medium 72 h before each experiment. The axenic conditions were maintained by carrying out experiments under a class II laminar flow hood to avoid biotic contamination.

2.1.2. FLG suspension

2.1.2.1. Synthesis. The FLG was prepared (CIRIMAT) by an exfoliation process from expandable graphite flakes. This starting material, provided by Asbury Carbons (Ref. 3772), is a graphite of natural origin which has been industrially treated with acids and using strong oxidizing agents as catalysts, before being washed and dried. In this way, acidic compounds are intercalated between graphene sheets. This enables a later expansion of the material using a sudden thermal treatment.

Here, this thermal expansion was carried out from 2.6 g of expendable graphite fakes. Batches of 200 mg (in 55 mL crucibles) were thus placed 4 min in an open furnace maintained at 900 °C under air, before being removed for cooling at room temperature. The 810 mg resulting expanded graphite were dispersed in 4 L of propan-2-ol to reach a 0.2 g L^{-1} nominal concentration. The mechanical exfoliation was carried out from this suspension. First, it was homogenized with a shear mixer (Silverson L5M) for 15 min at 8000 RPM by batches of 1 L. Besides, it underwent a probe sonication for 90 min at 50% amplitude (Vibra cell 75042, 13 mm-diameter probe, 500 W, 20 kHz) by batches of 200 mL.

A size selection of the particles was then realized by centrifugation at 800 G. Immediately prior to the centrifugation, the 200 mL batches were submitted again to a 4 min sonication at 50% amplitude in order to redisperse agglomerates which may have formed during the storage of the suspensions. The batches were then submitted to centrifugation for 45 min in 0.6 L flasks (Thermofisher scientific Heraeus Megafuge 40, rotation acceleration = 9, rotation deceleration = 3).

The collected supernatant was filtered on cellulose nitrate membranes (45 mm diameter, 0.45 μm pore size) and washed with deionised water (1 volume of deionised water per volume of suspension). The membrane with the FLG deposit was placed in deionised water in a 10 mL flask and bath sonicated for 10 min (Elmasonic S30H, 280 W) in order to fully recover the FLG from the membrane. This FLG suspension was finally frozen and freeze-dried (Christ Alpha 2–4 LSC) leading to a final weight of 19.8 mg which corresponds to a 0.8 wt % global yield.

FLG was dispersed in SPE medium, bath sonicated for 10 min (Elmasonic S30H, 280 W) and autoclaved. Dilutions were then

carried out from this suspension for the algal test and microscope observation. Before pipetting, the initial suspension was again homogenized by sonication for 2 min using a BRANDSON digital sonifier S-250D with a 1/8 inch Tapered Microtip (200 W; amplitude: 35% 5s/2s) to prepare four homogenous intermediary FLG suspension at 0.167, 1.67, 16.7 and 83.5 mg L^{-1} used. These intermediary dilutions permitted to prepare the experimental device with the real concentrations 0.1, 1, 10 and 50 mg L^{-1} for the exposure. A last sonication was carried out just before adding FLG suspension in the exposure medium.

2.1.2.2. Characterization. The morphology of the dried particles and their size were characterized by Transmission Electronic Microscopy (TEM, JEOL JEM 1400). A very small fraction of the powder was dispersed for 10 min by ultrasonic bath in ethanol, and few drops were deposited on a TEM grid (Lacey carbon). The structure was controlled by RAMAN spectroscopy on a Labram-HR800 (Horiba) using a laser at 633 nm in confocal mode (×100 magnification, 100 μm hole, diaphragm D1, 20 s exposition, 10 accumulations). The chemical composition was analyzed by XPS (Kα ThermoScientific, monochromatic Al-Kα source).

To avoid misinterpretations in the potential FLG toxicity investigation [37], the analysis of macro-, micro-nutrient and trace elements were conducted by incubation of 50 mg L^{-1} of FLG in the culture medium under stirring during 144 h. The mixture was filtered at 0.1 μm on a Minisart® high flow polyethersulfone membrane (SARTORIUS-STEDIUM). Elements were quantified by inductively coupled plasma-optic spectrometry (ICP-OES, Agilent-7500ce, Agilent Technologies, Palo Alto, CA) to check for a potential release by FLG.

2.2. Exposure conditions

The experimental device used in this study was the same as the one previously described by Pouvreau et al. [38] and Verneuil et al. [36] to distinguish the shading effect from the total effect (combined effect of direct exposure and shading) on algae exposed to nanoparticles. Experiments were carried out using experimental device where two 12-wells plates (COSTAR®-3513, Corning Incorporated, Corning, NY) were superimposed on each other with a black film stuck around the wells on the upper one. The plates were surrounded by Parafilm® to avoid medium evaporation, and then placed in an open-topped opaque box to allow light perception by diatoms only from the top aperture of wells.

Before the beginning of the exposure to FLG, lower plates of each device were inoculated with 1 mL of algal culture (2.5×10^5 cells. mL^{-1}) to establish the algal biofilm. These plates were then shaken in a culture room for 24 h of light at 120 μE. Then, to test the Total effect, 1.5 mL of a dispersed suspension of nanoparticles, at the appropriate concentration, were added into each well of the lower plates in order to obtain a final volume of 2.5 mL per well (corresponding to time 0). The final FLG concentrations were respectively 0.1, 1, 10, and 50 mg L^{-1} (FLG_{50mg}). For the Shading effect test, 1.5 mL of FLG suspensions were placed in each well of the upper plates only. The wells which did not contain a final volume of 2.5 mL, were filled with SPE medium (2.5 mL in wells of the upper plate for the Total effect test and 1 mL in wells on the upper plate for the Shading effect test). Wells were monitored by sampling at 24, 48, 72 and 144 h. Each experimental condition was conducted in triplicate.

2.3. Effect of FLG on N.palea growth and viability

At the end of the incubation time, the contents of triplicate wells were scraped and homogenized. Algal concentrations were assessed performing two counts per well using a Malassez cell counter. Like in Verneuil et al. study [36], the growth rates (r) was calculated from the following equation (with $n_0 = 1 \times 10^5$ representing the number of cells per mL at the beginning of the exposure and n_x = the number of cells per mL after x hours of exposure to FLG).

$$r = \frac{n_x - n_0}{n_0}$$

Algal viability was determined at 48 h of exposure to FLG suspensions using SYTOX Green® marking (Molecular Probes, Inc., Eugene, OR) [39] generally used on bacteria [40] but also on diatoms [41]. After scrapping, cells were incubated 10 min in SYTOX Green® (100 nM) and then observed using a fluorescence microscope (BX-41, Olympus, Center Valley, PA) equipped with an Hg lamp (U-LH100HG, Olympus, Center Valley, PA) using a 470–490 nm/520 nm excitation/emission filter and a 500-nm dichromatic filter (U-MNB2, Olympus, Center Valley, PA). All injured or dead cells present an apparent green fluorescence of the nucleus whereas intact cells do not present any fluorescence (Invitrogen, Molecular Probes, SYTOX® Green Nucleic Acid Stain). The rate of dead cells was determined by the following equation (T represents the rate of dead cells, n_{48} = the total number of cells counted 48 h after the beginning of the exposure and n_d = the number of counted dead cells)

$$T(\%) = \frac{n_d}{n_{48}} * 100$$

2.4. Effect of FLG on photosynthetic activity

In agreement with Verneuil et al. [36], the photosynthetic active radiations (PAR) received by *N. palea* were measured at 48 h of exposure, using a light-meter (Li-250 A light meter equipped with Li-COR Quantum sensor; Li-COR Biosciences, San Diego, CA). Before the measurement, the agitation of culture flasks was stopped and the sensor was placed between the two plates for each condition for the Shading test, and under the lower plate in Total exposure conditions. Measurements for the control condition were carried out under and between the two plates to compare PAR values in FLG exposure to the respective control value.

Pulse Amplitude Modulated fluorimetry (PAM) was carried out to assess photosynthetic activity of diatoms exposed to FLG using a Phyto-PAM (Heinz Walz GmbH, Effeltrich, Germany). After a strong light pulse, the photosystem II quantum yield (PSII) was obtained from fluorescence yield measured just before the saturation pulse and the maximal fluorescence yield. Then, the photosystem II quantum yield is the ratio of emitted photons and photons absorbed by chlorophyll after the illumination pulse. When the quantum yield is close to 0, photosystem II is strongly altered and photosynthetic activity is totally inhibited. This value rises when the photosystem II activity is increased (Phytoplankton Analyzer PHYTO-PAM and Phyto-Win Software V 1.45, System Components and Principles of Operation). Measurements were done 48 h after the beginning of the exposure to FLG for each triplicated condition, and after dark conditioning of well plates for approximately 10 min. A measurement was carried out on wells containing only FLG_{50mg} to control the impact of FLG on the Phyto-PAM measurement.

2.5. Assessment of FLG-Diatoms interaction and microscopy observation of N. palea biofilms

The interaction between FLG and diatoms was investigated at 6, 24, 48 and 144 h of exposure to FLG_{50mg} by combining (i)

macroscopic observation of the wells, (ii) optical density measurements after sampling the water column, (iii) observation of the biofilm by stereomicroscopy, and (iv) observation of the biofilm by scanning electron microscopy (SEM).

A first macroscopic observation was carried out using a stereo microscope (SZX2-ILLT, Olympus Corporation, ×8 and ×56) to photography the full wells in the presence and in the absence of diatoms. After this, 1 mL of the supernatant (fraction called S, Fig. 1) was sampled to assess the FLG concentration in the shallow-depth part of the water column and the rest of the contents (fraction of 1.5 mL called S′) was sampled to evaluate the sedimentation of FLG above the diatoms biofilm. The wells were rinsed once with 1 mL of SPE medium and a second macroscopic observation of the bottom of wells was performed. The percentage of FLG in the three compartments was calculated as follows (where $\%S$ and $\%S'$ represent the percentage of FLG quantity in the respective fractions S and S′, OD_S, $OD_{S'}$ and OD_i are the OD_{800} value for the respective fractions S and S′ and for the total fraction of the well, V_s and $V_{S'}$ represent the volume of the respective fraction sampled S and S′, V_{tot} is the total volume of the wells = 2.5 mL, and % FLG stuck represents the percentage of FLG stuck in the biofilm):

$$\%S = \frac{OD_S * V_s}{OD_i * V_{tot}} \qquad \%S' = \frac{OD_{S'} * V_{S'}}{OD_i * V_{tot}}$$

$$\%FLG\ stuck = 100 - \%S - \%S'$$

The fraction S and S′ removed from wells prior to stereomicroscopy were preserved for measuring the optical density measurement as previously described to assess the fate of carbon nanoparticles in the presence of algae [42]. To avoid chlorophyll absorbance, the optical density was measured at 800 nm (OD_{800}) in the fraction S and S′ at 6, 24, 48 and 144 h of exposure to FLG_{50mg} using a spectrophotometer (Secomam Anthelie UV/Visible Light Advanced Spectrophotometer) for each condition. This OD_{800} measurement was also carried out with only FLG_{50mg} in wells to confirm the absence of adherence of nanoparticles at the bottom of the wells. These measurements allowed to characterize the nanoparticles behavior in wells.

After collecting fractions S and S′, the wells were rinsed once with 1 mL of SPE medium and a second macroscopic observation of the bottom of wells was performed by stereomicroscopy. The collected images were analyzed with the "ImageJ" software ("ImageJ" 1.45s, Wayne Rasband, National Institute of Health, USA) using the "Analyze Particles" module to quantify the area covered by FLG adhered on diatoms biofilm. Wells containing only diatoms (0 mg L^{-1} of FLG) were considered to fix the threshold value for FLG detection with ImageJ software.

At the cellular level, interaction between FLG nanoparticles and diatoms biofilm was observed for each condition by both light microscopy and SEM. For SEM analysis, glass coverslip were placed at the bottom of wells before inoculating cultures and exposing diatoms to FLG_{50mg} for 48 h. Then, samples were fixed and colored with Alcian blue (Sigma-Aldrich, Paris, France) directly in the wells following the Erlandsen's et al. [43] protocol with some modifications also used in earlier work by Verneuil et al. [36]. First, an incubation of 24 h in a solution of 0.1% Alcian blue in acetic acid (0.5 M), paraformaldehyde (2%), and glutaraldehyde (2%) buffered using sodium cacodylate (0.15 M) permitted samples fixation directly in wells. Then, wells were rinsed with a cacodylate buffer (0.15 M). A second fixation step consisted in a 2 h incubation in a solution of cacodylate buffer containing potassium ferro-cyanide (1.5%) and OsO_4 (1%) was conducted. Then, samples were rinsed again and dehydrated in an ascending ethanol gradient [50, 70, 80, and 95%] each for 10 min and twice for 15 min in ethanol 100% before drying with N_2. Glass coverslips were then placed on SEM mounts and platinum coated before observation (JEOL JSM-6700F, 3 kV, detection mode: Secondary Electron Imaging).

2.6. Statistical analysis

All statistical analysis were applied at a maximum level of 5% by a one-way analysis of variance (ANOVA) implemented using the statistical open source software "R" (SSR; R Development Core Team 2012, Bio-RAD, Charlottesville, VA) to detect a significant difference between the different conditions for the growth test, viability test and PSII quantum yield measures. This analysis was followed by Tukey HSD *post hoc* test to determine which conditions were different from the others. If data did not follow a normal distribution, equivalent non-parametric tests were run (Kruskal-Wallis analysis of variance followed by Kruskal mc test *post hoc*). Thus, to estimate a correlation between FLG concentration and PSII quantum yield, a Kendall test was run. Furthermore, a correlation between PAR and the cellular density was tested to exclude the influence of the presence of diatoms at the bottom of wells on the PAR measurement running a Kendall test.

3. Results

3.1. Characterization of FLG suspension

Fig. 2 shows an example of FLG nanoparticles. From both Transmission Electronic Microscopy) TEM and XRD measurements (confirming an interlayer distance of 0.335 nm) the number of layers was estimated to be between 5 and 10.

A small D band was observed at 1330.1 cm^{-1} in Fig. 3. Its relative intensity ($I_{D/G} = 0.1$) was especially low in comparison to what is typically described in the literature using other routes (for example stronger oxidizing treatments of graphite followed by reduction). The low FWHM (17 cm^{-1}) of the G peak at 1580.4 cm^{-1} also confirmed the good structural quality of this material.

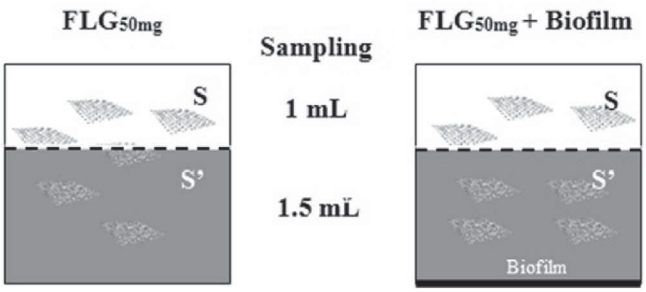

Fig. 1. Schematic representation of FLG distribution between the three compartments in wells: fractions S and S' in the water column and fraction of FLG stuck on the biofilm.

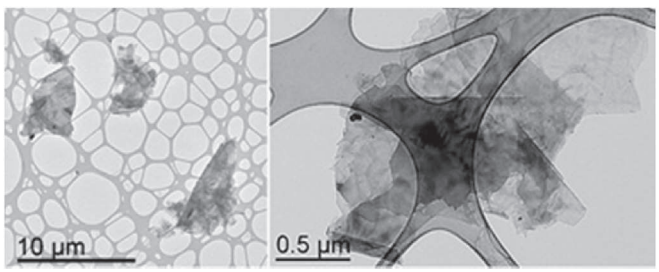

Fig. 2. Transmission Electronic Microscopic micrography of FLG after drying and dispersing in ethanol.

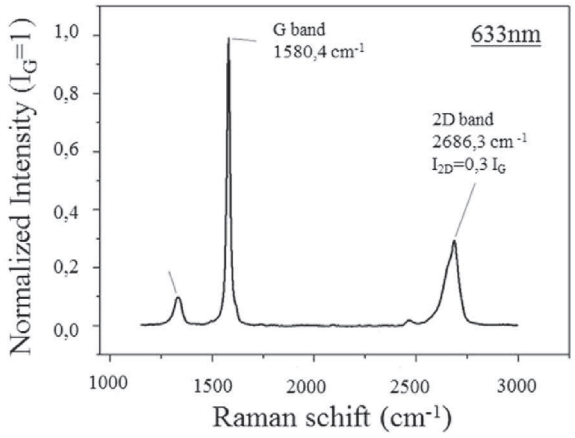

Fig. 3. Raman spectrum of dried FLG.

The atomic composition of the surface was mainly: C = 94.5 at. % (284.1 eV), O = 4.0 at. % (532.0 eV) (Fig. S2). Si accounted for 1.5 at. %, although nothing in sample preparation could explain the presence of this element. However, it may originate either from the adhesive carbon tape used to prepare the sample for XPS analysis, or from SiO_2 coming from the glassware used for sample processing. Oxygen may also come from residual humidity, XPS is also very sensitive to this.

The ICP-OES analysis did not reveal any difference between the medium culture without nanoparticles and the medium culture incubated with FLG_{50mg} (Table 1), demonstrating the absence of release of metallic ions by FLG. Furthermore, no absorption of nutrients by FLG were demonstrated in this study which is a current observation in the bioassays testing nanoparticles of the graphene family nanomaterial [3].

Table 1
Quantity of the different elements measured by ICP-OES analysis in the medium culture in the absence and in the presence of FLG_{50mg}. ND = not detected.

Elements quantified	Medium culture (ppm)	Medium culture + FLG_{50} (ppm)
Medium culture elements		
Si	10.41 ± 0.26	12.55 ± 0.04
Na	25.92 ± 0.33	27.03 ± 0.06
Ca	9.36 ± 0.14	9.74 ± 0.07
Mg	2.27 ± 0.03	2.33 ± 0.02
S	2.98 ± 0.07	3.20 ± 0.02
K	4.42 ± 0.02	4.44 ± 0.05
P	1.55 ± 0.06	1.512 ± 0.002
B	0.43 ± 0.01	0.539 ± 0.019
Mn	0.044 ± 0.001	0.047 ± 0.002
Fe	0.27 ± 0.01	0.1435 ± 0.0008
Mo	ND	ND
Zn	0.008 ± 0.003	0.018 ± 0.002
Co	0.0018 ± 0.0001	0.0018 ± 0.0001
Se	ND	ND
V	ND	ND
Elements quantified	Medium culture (ppm)	Medium culture + FLG_{50} (ppm)
Trace elements		
Cd	0.0001 ± 0.0001	ND
Ag	ND	ND
Al	ND	ND
As	ND	ND
Ba	ND	ND
Be	ND	ND
Cr	ND	ND
Li	ND	ND
Ni	ND	ND
Pb	ND	ND
Rb	ND	ND
Sb	ND	ND
Sc	ND	ND
Se	ND	ND
Sr	ND	ND
Ti	ND	ND
Tl	ND	ND
U	ND	ND

3.2. FLG effects on N. palea growth and viability

Fig. 4 shows the growth kinetics curve of *N. palea* determined by cellular counting from 24 h to 144 h of exposure. For each experiment, growth rate was determined at 48 h, corresponding to the end of the exponential growth phase, and at 144 h of exposure, corresponding to the stationary period.

Diatoms growth rate calculated for the Total exposure and Shading conditions at 48 h and 144 h are represented in Fig. 5a and b, respectively. After 48 h of direct exposure (Total effect), FLG caused a decline of diatoms growth for both exposure conditions. The decrease in growth rate was significant only for diatoms exposed to FLG_{50mg} suspensions (Fig. 5a) (p-value<0.05) reaching a minimum value of 0.3 ± 0.2. After 144 h of FLG exposure (Fig. 5b), the inhibition totally disappeared whatever the tested concentrations (0.1–50 mg L^{-1}). Then, at the end of the experiment, the average diatoms growth rate was about 9.2 ± 0.3. In the case of the Shading test, the growth rate was significantly lower than control only for the culture exposed to FLG_{50mg} (48 h: 5.1 ± 1.4, 144 h: 10.8 ± 0.2) at respectively 48 h (2.1 ± 0.4) and 144 h (6.5 ± 1.4) of FLG exposure. Shading effect at lower concentrations had no significant impact on diatoms growth.

Fig. 6 shows the proportion of non-viable cells determined using SYTOX Green® staining of dead cells. This graph outlines a similar impact, although not significant, of the toxicity between 0.1 and 10 mg L^{-1}. In the control conditions, 2.9 ± 1.6% of the cells were non-viable, which was consistent with mortality values cited by Verneuil et al. [36] in similar incubations. At FLG_{50mg} exposure, the viability test revealed a significant (p-value<0.05) increase in toxicity with a diatoms mortality around 22.2 ± 2.2%.

3.3. Effect of FLG suspension on photosynthetic yield and PAR

PAR was measured at 48 h of FLG exposure (Fig. 7). In the control condition, PAR was clearly higher than other study where diatoms are exposed to 45 μE [44] or 24 μE [36]. For both Total and Shading

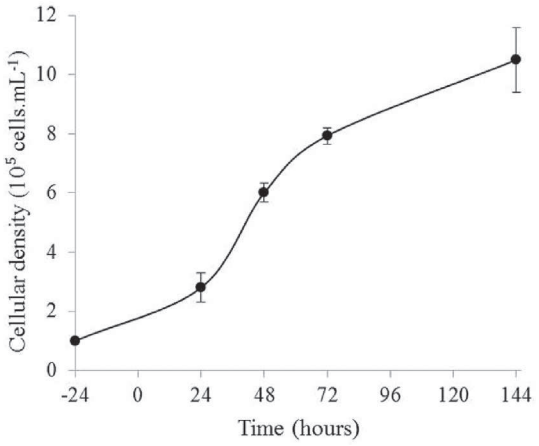

Fig. 4. Growth kinetic curve of N. palea control culture in SPE medium. Diatoms counting were carried out in Malassez cell at 24, 48, 72 and 144 h of growth. Error bars represent standard errors of the mean of 3 separate experiments.

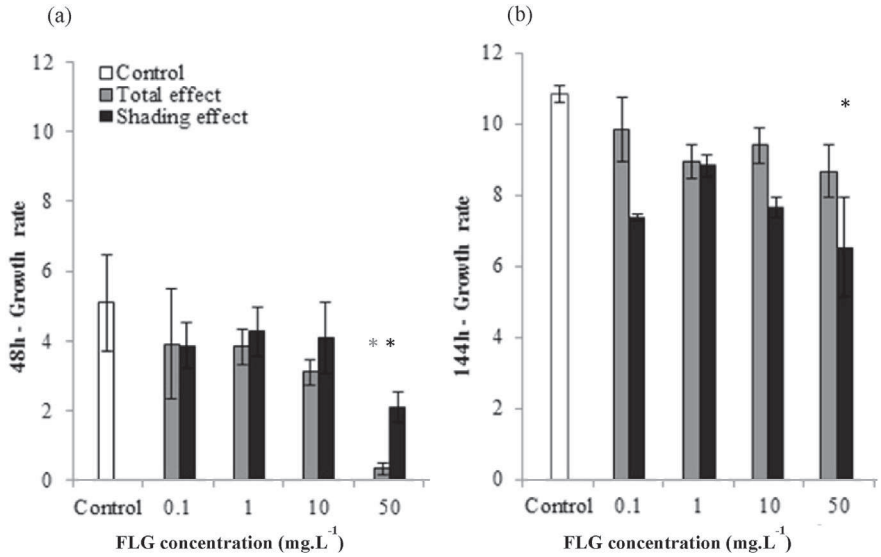

Fig. 5. Growth rate (r) of N. palea after 48 h (a) and 144 h (b) of FLG exposure for total effect test (grey bars) and shading effect test (black bars). (*) indicates significant difference ($p < 0.05$) between the different concentrations tested. Error bars represent standard errors of the mean of 3 separate experiments.

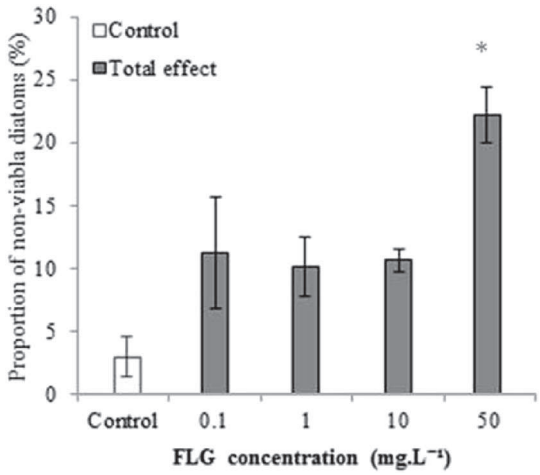

Fig. 6. Proportion of non-viable diatoms for total exposure test at 48 h of FLG exposure. (*) indicates significant difference ($p < 0.05$). Error bars represent standard errors of the mean of 3 separate experiments.

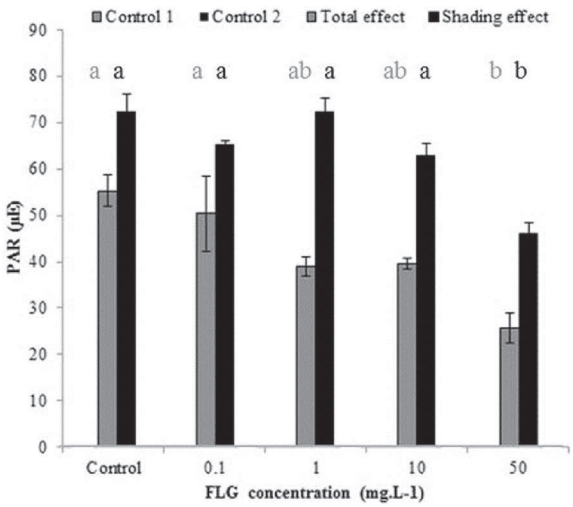

Fig. 7. Photosynthetic Active Radiation measured for the total exposure test (grey bars) and the shading test (black bars) at 48 h of FLG exposure. Groups with the same letter are not significantly different (p-value>0.05). Error bars represent standard errors of the mean of 3 separate experiments.

effect experiments, PAR decreased with the FLG concentration tested. Light intensity measured in shading condition was always higher than in total exposure due to the position of the sensor during the measurement which was placed between the two wells plates for the Shading test to assess exactly the shading provided by FLG. For total exposure, PAR decreased significantly from exposure to 50 mg L^{-1} of FLG with a PAR value of 25.7 ± 3.3 µE compared to the control 1 which exhibited a PAR value of 55.3 ± 3.4 µE. This decrease was also observed in shading condition where PAR remained stable from 0.1 to 10 mg L^{-1} and showed a significant decline only at 50 mg L^{-1} of FLG (46.0 ± 2.5 µE for FLG_{50mg} and 72.3 ± 3.9 µE for the control 2).

Fig. 8 depicts the PSII quantum yield measured at 48 h of FLG exposure. Control cultures presented a PSII quantum yield of 0.6 ± 0.1 comparable to values found in the literature (around 0.50) [45]. The absence of impact of the presence of FLG on the PSII measurement was verified (data not shown). PSII quantum yield measured in total exposure conditions showed a slight decrease in chloroplast integrity from 0.1 to 10 mg L^{-1} of FLG where diatoms exposed to this range of concentration exhibited an average PSII quantum yield of 0.6 ± 0.1. A significant decrease in PSII quantum yield was observed only for diatoms exposed to FLG_{50mg}. Thus, a significant negative correlation between PSII quantum yield and FLG concentration ($\tau = -0.57$; $Z = -2.78$; p-value<0.05) was observed in the total exposure test. In shading condition, no significant difference in PSII quantum yield was observed between control and treated diatoms regardless of FLG concentration. PSII quantum yield values remained stable during the experiment for diatoms exposed from 0.1 to 10 mg L^{-1} of FLG, except for diatoms exposed to FLG_{50mg}, with an average of 0.7 ± 0.0.

The interaction of FLG with the algal biofilm was investigated at 6, 24, 48 and 144 h of FLG_{50mg} exposure, using a stereo microscopy and SEM. This interaction was first quantified by monitoring FLG adhesion onto biofilm using stereo microscope, OD_{800} and PAR

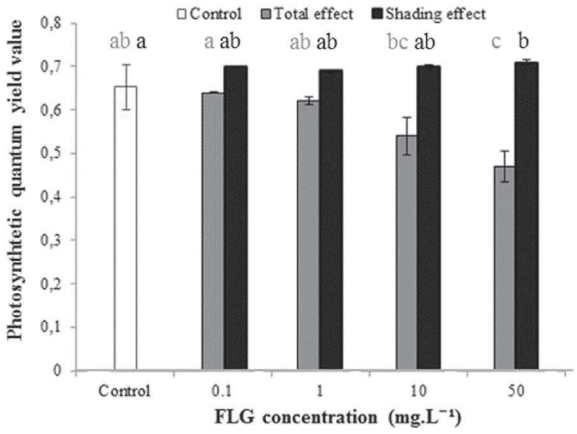

Fig. 8. Photosystem II quantum yield of N. palea exposed to the total effect (grey bars) and to shading effect (black bars) at 48 h of FLG exposure. Groups with the same letter are not significantly different (p-value>0.05). Error bars represent standard errors of the mean of 3 separate experiments.3.4. Quantification of FLG interaction with algal biofilm.

(data not shown). Fig. 9 shows examples of collected stereomicroscopy images of FLG_{50mg}. These images allowed to observing the size and the structure of the agglomerates of nanoparticles in the absence (Fig. 9a and b) or presence of diatoms (Fig. 9c and d). In the absence of diatoms, the nanoparticles were agglomerated in the water column in the center of the wells without any sign of adhesion at the bottom of the wells. In the presence of diatoms, nanoparticles formed numerous scattered agglomerates at the bottom of wells onto the biofilm.

Fig. 10 shows examples of collected SEM images of *N. palea* in control culture (Fig. 10a) and in cultures exposed to FLG_{50mg} (Fig. 10b–d). SEM allowed better observation at higher magnification of algal biofilm and the interaction with FLG at 48 h of exposure. SEM images evidenced the high affinity of FLG nanoparticles for the EPS. These images show that FLG nanoparticles were included in the EPS network (red arrows). Few FLG were also found directly on the surface of cells. The high magnification of SEM images allowed observing that FLG size was too large to enter into the cells by the pores of the frustules.

Fig. 11a and b shows examples of pictures analyzed using "ImageJ" software at 6 h and 144 h of FLG_{50mg} exposure where a significant difference could be observed in the quantity of spot of nanoparticles stuck at the bottom of wells. The quantification of FLG adhesion onto the algal biofilm by densitometry analysis is shown in Fig. 11c (represented by white points). An increase in FLG adhesion at the bottom of wells was observed from 5.8 ± 0.6% at 6 h to 18.0 ± 0.8% covering at 144 h in the presence of diatoms. Preliminary microscopic observations allowed verifying the absence of algae in the water column (data not shown).

The FLG concentrations in the two different fractions of the water column (S and S') measured by optical density and the deduced concentration of FLG stuck on the biofilm were expressed in relative percentage of FLG quantity. The dynamic of the FLG quantity in these three different compartments is presented in Fig. 11c. In the absence of diatoms, FLG quantity values indicated that FLG declined at shallow depth (fraction S) while it accumulated in the bottom of wells (fraction S'), but did not adhere to the plate. After 6 h, FLG in the bottom fraction of the well already accounted for 95.3 ± 0.4% of the total FLG quantity against 60% as the theoretical initial value. These data indicate that FLG underwent a sedimentation process within the water column, without any strong interaction with the plastic at the bottom of the well. In the presence of diatoms, FLG also sedimented, but in that case, FLG accumulated in the biofilm rather than in the bottom fraction of the water column (S'). Indeed, the amount of FLG stuck to the biofilm reached 71.4 ± 0.4% after 6 h and more than 98% at 144 h. At this time, the FLG in the water column was not detectable by OD_{800} measurement. These results confirmed data derived from ImageJ analysis.

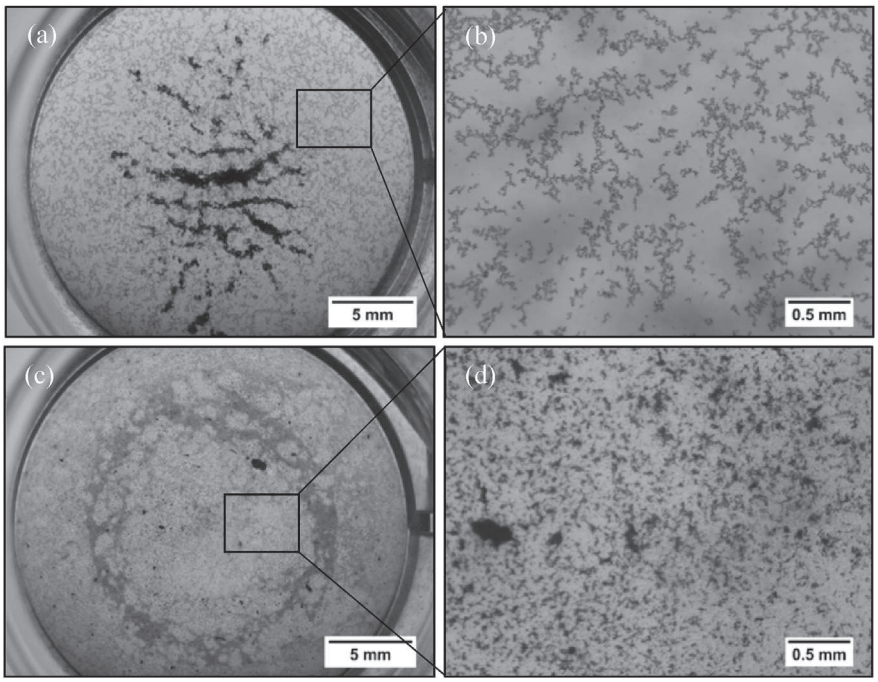

Fig. 9. Examples of collected images at stereo microscopy of full wells containing FLG_{50mg} without N. palea culture in large view (a) and in magnified view (b), and with N. palea culture in large view and (c) in magnified view (d) after 144 h of exposure.

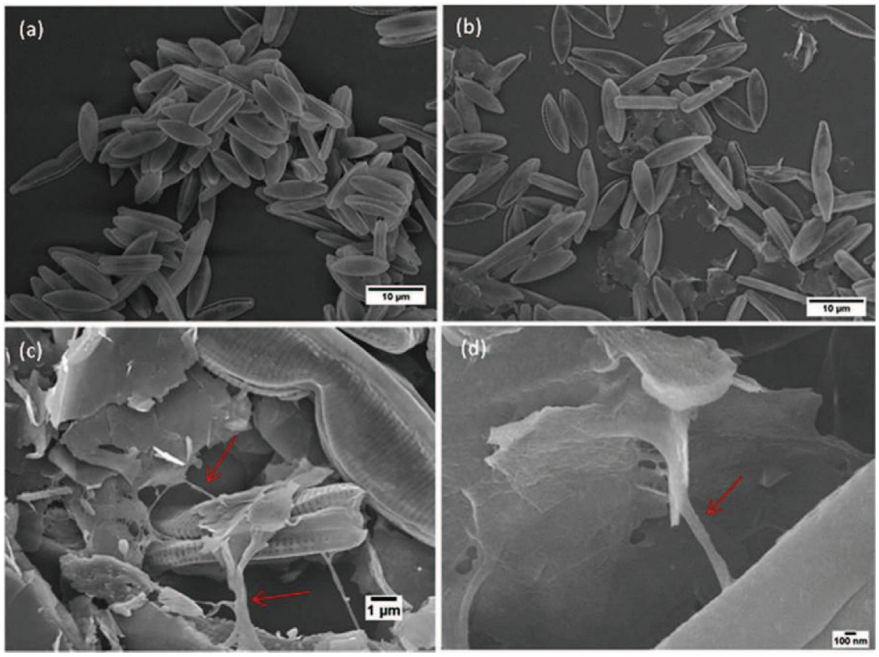

Fig. 10. Scanning electron microscopy images of N. palea at 48 h of growth in control culture (a) and in culture exposed to FLG_{50mg} (b–d). Red arrows indicate the EPS network secreted by diatoms. (A colour version of this figure can be viewed online.)

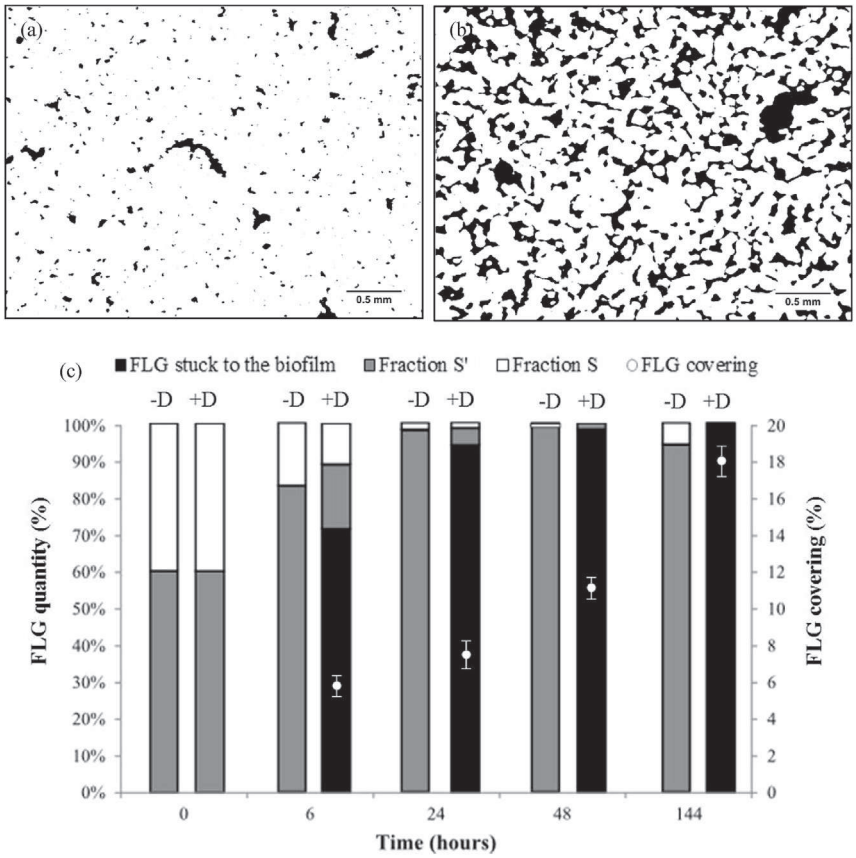

Fig. 11. Examples of pictures analyzed with "ImageJ" showing FLG at the bottom of wells after 6 h (a) and 144 h (b) of FLG_{50mg} exposure. FLG distribution derived from the OD_{800} measures between the different fractions: fraction S (measured, white bars), fraction S' (measured, grey bars) and FLG stuck on the algal biofilm (estimated, black bars) in the absence (-D) and in the presence (+D) of diatoms at the beginning (0 h) (theoretical value), 6, 24, 48 and 144 h of FLG_{50mg} exposure (c). FLG_{50mg} percentage covering at the bottom of wells derived from image analysis is represented by white dots (c). Error bars represent standard errors of the mean of 3 separate experiments.

4. Discussion

The aim of this study was to assess the global response of *N. palea* exposed to FLG measuring several standard endpoints (such as the growth rate, the algal mortality and membrane integrity) combined with a more original approach to characterize the and the interaction between the algal biofilm and nanoparticles. In this study a particular interest was assigned to the different effects of FLG distinguishing the shading effect which is a potential part of the total effect of FLG on *N. palea*.

4.1. Effect of total exposure on diatoms growth and viability

Diatoms growth and mortality were assessed for the Total and Shading effect test simultaneously. When cells were directly in contact with nanoparticles (Total effect), the exposure to FLG induced a dose-dependent inhibition which was significant only for diatoms exposed to 50 mg L^{-1} of FLG. Furthermore, the analysis of cell viability revealed a high percentage of mortality only for diatoms in contact with FLG_{50mg} at 48 h. These results suggest a real toxicity of FLG suspensions from 50 mg L^{-1}. Alterations of the photosynthetic quantum yield (PSII yield) confirmed this toxicity leading to a significant decrease of 28% of photosynthetic activity for diatoms exposed to the highest concentration (50 mg L^{-1}). Nevertheless, this decline is not due to a shading effect because in this condition quantum yield was not affected (Fig. 8). This inhibitory response of diatoms PSII yield could be caused by the contact with FLG nanoparticles as shown by the negative correlation between PSII yield and FLG concentration observed only in direct exposure, meaning a negative effect of FLG on photosynthetic activity. These results could suggest that direct physical interaction between FLG and diatoms lead to frustule damages and a loss of plasma membrane integrity. These physical disruptions were already observed in presence of graphene oxide and CNTs on *E. coli* [46,47], observed with SEM and TEM, leading to cell damages and morphological alterations.

Thus, OD_{800} values in the absence of diatoms allowed to confirm that FLG nanoparticles sediment at the bottom of the wells leading to a contact with the biofilm. This contact may be at the origin of toxic effects on cells at high concentration. In view of the dimensions of FLG, a shearing effect could be hypothesized. Then, chloroplast alterations and inhibition of PSII yield could be a consequence of diatom cell damages.

The FLG toxicity, like other nanoparticles may result from numerous factors: damage by direct contact as previously observed [48] and mentioned in a previous paragraph, but also reactive oxygen species (ROS) production [49,50]. ROS generation can be caused either by direct contact and/or indirect effects, associated with the physico-chemical properties of the materials, the functionalization of the surface and/or the release of toxic elements, involved in the nanomaterial synthesis processes. In many cell types, ROS generation is generally associated to plasma membrane disruption and mitochondria alteration [50]. Today, little is known about toxicity pathways for graphene in general and FLG in particular. However, it has been suggested that because of their similarity to carbon nanotubes, oxidative stress may be an important pathway in the graphene family effects [3].

Several works focusing on the study of carbon nanoparticles revealed that their toxicity was associated with the presence of exogenous compounds as metal ions, used as nanoparticles catalyzer for example [51–53]. FLG was not grown catalytically and do not contain residual metal catalysts. However, a related contamination due to its mode of dispersion by ultrasonic probe may be at the origin of the presence of metals. So, the analysis of numerous trace elements were conducted by incubation of 50 mg L^{-1} FLG in the culture medium under stirring during 144 h. The absence of toxic metallic ions (Table 1) demonstrated that growth inhibition and toxicity were not caused by metal contamination. One of the characteristics of FLG materials is their high surface area. FLG is described as a potent sorbent for a wide variety of small molecule solutes in a physiological fluid. Adsorption on carbon surfaces is possible for molecules with high lipophilic degree, molecules with conjugated π bonds or molecules with positive charge. In this last case, the biological consequences could be a micronutrient depletion [54]. The analysis of nutrient composition of diatom culture medium in presence and absence of 50 mg L^{-1} FLG has shown no significant differences. So, in this work, growth inhibition and cell mortality at 48 h were not associated to release and/or sorption processes but support a direct effect of FLG on diatom cells.

The growth recovery observed at 144 h of total exposure might signify a decline or an absence of toxic effect of FLG on diatoms at this time. These results support the hypothesis that the pressure of the toxic agent is mitigated. Growth recovery was also observed by Verneuil et al. [36] when diatoms were exposed to CNTs. These results suggest the implementation of a protection process limiting interaction with FLG allowing the growth over the biofilm containing the nanoparticles. These results underline the capacity of diatoms to recover their growth even after a strong initial perturbation. This capacity can be related with the biofilm development. Brouwer et al. [55] reported that EPS production had a major role in the biostabilization, reducing potential for erosion, and the matrix can be considered as a microbial recycling storage. But it is not the only benefits of EPS matrix, which can confer a protection against trace elements and biocides even at high concentrations [56].

4.2. Shading effect of FLG

In shading condition, growth inhibition was observed at 48 h of FLG_{50mg} exposure without a growth recovery at 144 h. These results revealed that the presence of FLG_{50mg} in the upper plate strongly inhibited diatoms growth until 144 h of exposure. In this condition, an effect which is not a contact one is stated. An exposure to FLG_{50mg} promotes a shading effect which is too high and does not permit a growth recovery because (i) of a significant PAR deficit (Fig. 7), and (ii) cells and EPS are not in contact with nanoparticles and then cannot interact with them. As shown by Pouvreau et al. [38] when the light intensity is not enough, the algal growth is altered. Therefore, growth inhibition observed in direct contact condition at 48 h of exposure is due to a combination of toxic and shading effect. Combined effects (contact and shading) on cell growth in presence of CNTs was also demonstrated by Long et al. [57] and Schwab et al. [58] on *Chlorella sp.* However, shading effect did not result in a significant diatom mortality even at the highest FLG concentration tested in the present study. Shading effect was also observed with the exposure of other brown algae such as *Fucus serratus* to carbon black nanoparticles [59].

Contrary to carbon nanoparticles, metal oxide nanoparticles can cause an opacification of the culture medium without shading effect on organisms reported [60,61]. The most studied nanoparticles were cerium dioxide (CeO_2) and titanium dioxide (TiO_2). These kinds of nanoparticles lead to milky suspensions and present an absorption spectra only in the UV-range [62]. Some cytotoxic effect of metal dioxide nanoparticles were demonstrated on green algae, daphnia and bacteria [63–65] but no toxic effect were observed on photosynthetic activity and no shading effect was recorded for CeO_2 nanoparticles on diatoms [66]. Overall, the shading effect seems to be specific to carbon nanoparticles, as a result of their black color. Thus, carbon-based nanoparticles appear to automatically promote shading effect on benthic and pelagic organisms. In this study, the results show that the shading did not significantly

alter the photosynthetic activity at low FLG concentrations. The photosystem II activity was slightly but significantly promoted at high FLG concentration only. The presence of TiO_2 or ZnO_2 nanoparticles was previously shown to increase the chlorophyll synthesis in several photosynthetic organisms [67,68] which can be considered as a response to a photo-induced stress. This shading can alter physiological activity of photosynthetic organisms such as the reproduction or the fertilization process. The increase of the photosynthetic activity in shading exposition suggest that *N. palea* invested more energy in chlorophyll synthesis which represent the main source of energy in these cells. In these conditions, the energy allocated to cell division was reduced.

4.3. Investigation of the interaction between diatoms biofilm and FLG suspension

The interaction between algal biofilm and FLG nanoparticles was investigated by microscopic observation but also by a monitoring of OD_{800} of the supernatant. Wells observations at FLG_{50mg} exposure has shown that, in the absence of diatoms, FLG nanoparticles were agglomerated in the center of the wells and did not adhere at the bottom of the plate even if a sedimentation phenomenon could be observed (Fig. 9a and b). Nevertheless, in the presence of diatoms, carbon nanoparticles formed numerous heterogeneous agglomerates stuck at the bottom of the wells (Fig. 11a, b, c). These observations support a real interaction between algal biofilm and nanoparticles, leading to the formation of large agglomerates of nanoparticles at the bottom of wells. Furthermore, FLG adhesion rate onto diatoms and the monitoring of OD_{800} in the water column suggested a transfer of FLG from the water column to the bottom of wells. As a result, most nanoparticles for the exposure concentration of 50 mg L^{-1} were found stuck at the bottom of the wells because of a strong interaction with algal biofilm. This sticking was not due to the adherence of nanoparticles alone at the bottom of wells. Furthermore, SEM observations (Fig. 10) provide an evidence of a strong agglomeration and adherence of FLG on the EPS network secreted by diatoms.

The data derived from the monitoring of FLG concentration in the water column and from microscopic observation were in agreement. The sedimentation process undergone by FLG in the water column, which was associated with the sticking promoted by EPS secreted by diatoms, as previously described [34].

It is well known that *Nitzschia palea* diatom species can be found in contaminated or eutrophic medium [69]. This species presents a strong resistance capacity which can be related with the biofilm production. It was reported that the secretion of EPS by the marine diatoms *Thalassiosira weissflogii* [70] increased in the presence of Ag nanoparticles and reduced its toxicity [71] suggesting that EPS can be involved in a detoxification process by this diatom. Furthermore, the secretion of polysaccharides in the medium seems to be a defense mechanism of algae against heavy metals [35,72]. More recently, Verneuil et al. [73] also demonstrated the role of EPS production in diatoms cultures exposed to CNTs. The authors reported the high proportion of hydrophobic proteins in EPS, which represent the primary part of extracted EPS. Otherwise, extracellular DNA was identified as another component of EPS during the biofilm development which can be a structuring element of algal biofilm [56,74]. Tong et al. [75] reported that the presence of extracellular DNA appears to play a role in the initial adhesion and the biofilm formation of *Reinheimera* sp. F8, *Pseudomonas* sp. FW1, *Microbacterium* sp. FW3 and *Serratia* sp. FW2 and especially during the exponential growth phase. A strong affinity between nucleic acids and graphene has been previously reported [3] and supports the possible involvement of extracellular DNA in EPS and FLG interaction.

5. Conclusion

Exposure of *N. palea* to FLG clearly promotes a negative cellular response at high concentration with a dose-dependent growth inhibition and an effective short-term toxicity. The frustule appears to be an efficient barrier preventing the FLG cellular uptake but it is not sufficiently resistant to the physical interaction, which can be a potential cutting effect, of FLG nanoparticles. In this paper, we demonstrated that the cytotoxicity is caused by a negative impact of both the direct contact of cells with nanoparticles but also a shading effect. This indirect effect was only observed with dispersed CNTs. Shading seems to be specific to carbon-based nanoparticles. EPS secretion appeared to be a key process in the response of diatoms resulting in the clarification of the water column. This process allows reducing contact opportunities between FLG and diatoms which can recover a normal growth after 144 h of exposure. Then, the clarification of the water column by *N. palea* results in physical interactions with FLG. To go further, an assessment of the composition of the EPS secreted while diatoms are exposed to different carbon-based nanoparticles could be the next step to determine the specificity of the response induced by *N. palea*. Beyond the proper response of *N. palea* to FLG exposure, our results have ecological implications. FLG sticking in the biofilm is likely to mitigate its ecotoxicity not only towards *N. palea* but also towards other organisms in aquatic ecosystems, including pelagic organisms. Despite the absence of toxic effects at low concentrations on *N. palea*, toxicity effects might occur for upper organisms in the food chain. Indeed, the sticking of FLG in the biofilm results in the concentration of nanoparticles in the biofilm which can be ingested by grazers. These organisms would be exposed to higher concentration which could lead to toxic effects.

Acknowledgments

We thank the financial support for this study provided by the French Ministry of Higher Education and Research (PhD grant No 2015–73). The research leading to these results has received funding from the European Union Seventh Framework Program under grant agreement No 604391 Graphene Flagship. We acknowledge the Common Service for Scanning Electron Microscopy of the University Paul Sabatier and Stephane Le Blond Du Plouy for his technical help.

Appendix A. Supplementary data

Supplementary data related to this article can be found at http://dx.doi.org/10.1016/j.carbon.2016.11.033.

References

[1] C.O. Hendren, X. Mesnard, J. Dröge, M.R. Wiesner, Estimating production data for five engineered nanomaterials as a basis for exposure assessment, Environ. Sci. Technol. 45 (2011) 2562–2569, http://dx.doi.org/10.1021/es103300g.
[2] J.Y. Bottero, M. Auffan, D. Borschnek, P. Chaurand, J. Labille, C. Levard, et al., Nanotechnology, global development in the frame of environmental risk forecasting. A necessity of interdisciplinary researches, Comptes Rendus - Geosci. 347 (2015) 35–42, http://dx.doi.org/10.1016/j.crte.2014.10.004.
[3] V.C. Sanchez, A. Jachak, R.H. Hurt, A.B. Kane, Biological Interactions of Graphene-family Nanomaterials: an Interdisciplinary Review, 2012, pp. 15–34, http://dx.doi.org/10.1021/tx200339h.
[4] N.K. Mahanta, A.R. Abramson, Thermal conductivity of graphene and graphene oxide nanoplatelets, 13th Intersoc. Conf. Therm. Thermomechanical Phenom. Electron Syst. (2012) 1–6, http://dx.doi.org/10.1109/ITHERM.2012.6231405.
[5] K.S. Novoselov, A.K. Geim, S.V. Morozov, D. Jiang, M.I. Katsnelson, I.V. Grigorieva, et al., Two-dimensional gas massless Dirac fermions graphene 438 (2005) 197–200, http://dx.doi.org/10.1038/nature04233.
[6] J.H. Seol, I. Jo, A.L. Moore, L. Lindsay, Z.H. Aitken, M.T. Pettes, et al., Two-dimensional phonon transport in supported graphene, Sci. (80) 328 (2010)

213–216, http://dx.doi.org/10.1126/science.1184014.
[7] D.A.C. Brownson, D.K. Kampouris, C.E. Banks, An overview of graphene in energy production and storage applications, J. Power Sources 196 (2011) 4873–4885, http://dx.doi.org/10.1002/9783527665105.ch5.
[8] Z. Wu, W. Ren, L. Wen, L. Gao, J. Zhao, Z. Chen, et al., in: Graphene Anchored with Co 3 O 4 Batteries with Enhanced Reversible, vol. 4, 2010, pp. 3187–3194, http://dx.doi.org/10.1021/nn100740x.
[9] C. Chung, Y.K. Kim, D. Shin, S.R. Ryoo, B.H. Hong, D.H. Min, Biomedical applications of graphene and graphene oxide, Acc. Chem. Res. 46 (2013) 2211–2224, http://dx.doi.org/10.1021/ar300159f.
[10] L. Feng, Z. Liu, Graphene in biomedicine: opportunities and challenges, Nanomedicine (Lond) 6 (2011) 317–324, http://dx.doi.org/10.2217/nnm.10.158.
[11] X. Hu, Q. Zhou, Health and ecosystem risks of graphene, Chem. Rev. 113 (2013) 3815–3835, http://dx.doi.org/10.1021/cr300045n.
[12] A. Nel, T. Xia, L. Mädler, N. Li, Toxic potential of materials at the nanolevel, Sci. (80) 311 (2006) 622–627, http://dx.doi.org/10.1126/science.1114397.
[13] A. Mottier, F. Mouchet, C. Laplanche, S. Cadarsi, L. Lagier, J. Arnault, et al., Surface area of carbon nanoparticles: a dose metric for a more realistic ecotoxicological assessment, Nano Lett. 16 (2016) 3514–3518, http://dx.doi.org/10.1021/acs.nanolett.6b00348.
[14] K. Savolainen, H. Alenius, H. Norppa, L. Pylkkänen, T. Tuomi, G. Kasper, Risk assessment of engineered nanomaterials and nanotechnologies—a review, Toxicology 269 (2010) 92–104, http://dx.doi.org/10.1016/j.tox.2010.01.013.
[15] R.H. Hurt, M. Monthioux, A. Kane, in: Toxicology of Carbon Nanomaterials: Status, Trends, and Perspectives on the Special Issue, vol. 44, 2006, pp. 1028–1033, http://dx.doi.org/10.1016/j.carbon.2005.12.023.
[16] P. Begum, R. Ikhtiari, B. Fugetsu, Graphene phytotoxicity in the seedling stage of cabbage, tomato, red spinach, and lettuce, Carbon N. Y. 49 (2011) 3907–3919, http://dx.doi.org/10.1016/j.carbon.2011.05.029.
[17] O. Akhavan, E. Ghaderi, Toxic. Graphene Graphene Oxide Nanowalls Against Bact. 4 (2010) 5731–5736, http://dx.doi.org/10.1021/nn101390x.
[18] W. Hu, C. Peng, W. Luo, M. Lv, X. Li, D. Li, et al., Graphene-based antibacterial paper, ACS Nano 4 (2010) 4317–4323, http://dx.doi.org/10.1021/nn101097v.
[19] O.N. Ruiz, K.A.S. Fernando, B. Wang, N.A. Brown, P.G. Luo, N.D. McNamara, et al., Graphene oxide: a nonspecific enhancer of cellular growth, ACS Nano 5 (2011) 8100–8107, http://dx.doi.org/10.1021/nn202699t.
[20] C. Pretti, M. Oliva, Pietro R. Di, G. Monni, G. Cevasco, F. Chiellini, et al., Ecotoxicity of pristine graphene to marine organisms, Ecotoxicol. Environ. Saf. 101 (2014) 138–145, http://dx.doi.org/10.1016/j.ecoenv.2013.11.008.
[21] X. Guo, S. Dong, E.J. Petersen, S. Gao, Q. Huang, L. Mao, Biological uptake and depuration of radio-labeled graphene by Daphnia magna, Environ. Sci. Technol. 47 (2013) 12524–12531, http://dx.doi.org/10.1021/es403230u.
[22] Y. Feng, K. Lu, L. Mao, X. Guo, S. Gao, E.J. Petersen, Degradation of 14C-labeled few layer graphene via Fenton reaction: reaction rates, characterization of reaction products, and potential ecological effects, Water Res. 84 (2015) 49–57, http://dx.doi.org/10.1016/j.watres.2015.07.016.
[23] G. Gollavelli, Y.-C. Ling, Multi-functional graphene as an in vitro and in vivo imaging probe, Biomaterials 33 (2012) 2532–2545, http://dx.doi.org/10.1016/j.biomaterials.2011.12.010.
[24] S. Scala, C. Bowler, Molecular insights into the novel aspects of diatom biology, CMLS 58 (2001) 1666–1673.
[25] T. Debenest, J. Silvestre, M. Coste, E. Pinelli, Effects of pesticides on freshwater diatoms, Rev. Environ. Contam. Toxicol. 203 (2010) 87–104, http://dx.doi.org/10.1007/978-1-4419-1352-4.
[26] P.F.M. Nogueira, D. Nakabayashi, V. Zucolotto, The effects of graphene oxide on green algae Raphidocelis subcapitata, Aquat. Toxicol. 166 (2015) 29–35, http://dx.doi.org/10.1016/j.aquatox.2015.07.001.
[27] A.B. Seabra, A.J. Paula, R. De Lima, O.L. Alves, N. Durán, Nanotoxicity of graphene and graphene oxide, Chem. Res. Toxicol. (2014) 27, http://dx.doi.org/10.1021/tx400385x.
[28] J. Zhao, Z. Wang, J.C. White, B. Xing, Graphene in the aquatic environment: adsorption, dispersion, toxicity and transformation, Environ. Sci. Technol. 48 (2014) 9995–10009, http://dx.doi.org/10.1021/es5022679.
[29] Z. Wang, Y. Gao, S. Wang, H. Fang, D. Xu, F. Zhang, Impacts of low-molecular-weight organic acids on aquatic behavior of graphene nanoplatelets and their induced algal toxicity and antioxidant capacity, Environ. Sci. Pollut. Res. 23 (2016) 10938–10945, http://dx.doi.org/10.1007/s11356-016-6290-4.
[30] P.G. Falkowski, J.A. Raven, Aquatic Photosynthesis, vol. Second edi, second ed., Princeton University Press, Princeton, 1997.
[31] W. Smith, A Synopsis of the British Diatomaceae: with Remarks on Their Structure, Functions and Distribution, and Instructions for Collecting and Preserving Specimens. 2. Van Voorst, 1956.
[32] C. Lancelot, S. Mathot, Biochemical fractionation of primary production by phytoplankton in Belgian coastal waters during short- and long-term incubations with 14C-bicarbonate, Mar. Biol. 86 (1985) 219–226, http://dx.doi.org/10.1126/science.333.6043.686.
[33] L.J. Stal, Microphytobenthos, their extracellular polymeric substances, and the morphogenesis of intertidal sediments, Geomicrobiol. J. 20 (2003) 463–478, http://dx.doi.org/10.1080/713851126.
[34] L.J. Stal, Brouwer JFC. De, Biofilm Form. by benthic diatoms their Influ. Stab. intertidal mudflats 12 (2003) 109–111.
[35] L.R. Andrade, R.N. Leal, M. Noseda, M.E.R. Duarte, M.S. Pereira, P.A.S. Mourão, et al., Brown algae overproduce cell wall polysaccharides as a protection mechanism against the heavy metal toxicity, Mar. Pollut. Bull. 60 (2010) 1482–1488, http://dx.doi.org/10.1016/j.marpolbul.2010.05.004.
[36] L. Verneuil, J. Silvestre, F. Mouchet, E. Flahaut, J. Boutonnet, F. Bourdiol, et al., Multi-walled carbon nanotubes, natural organic matter, and the benthic diatom Nitzschia palea, A sticky story 5390 (2014) 1–11, http://dx.doi.org/10.3109/17435390.2014.918202.
[37] E.J. Petersen, T.B. Henry, J. Zhao, R.I. MacCuspie, T.L. Kirschling, M.A. Dobrovolskaia, et al., Identification and avoidance of potential artifacts and misinterpretations in nanomaterial ecotoxicity measurements, Environ. Sci. Technol. 48 (2014) 4226–4246, http://dx.doi.org/10.1021/es4052999.
[38] J.-B. Pouvreau, E. Housson, Tallec L. Le, M. Morançais, Y. Rincé, J. Fleurence, et al., Growth inhibition of several marine diatom species induced by the shading effect and allelopathic activity of marennine, a blue-green polyphenolic pigment of the diatom Haslea ostrearia (Gaillon/Bory) Simonsen, J. Exp. Mar. Bio Ecol. 352 (2007) 212–225, http://dx.doi.org/10.1016/j.jembe.2007.07.011.
[39] S. Thakur, D.I. Cattoni, M. Nöllmann, The fluorescence properties and binding mechanism of SYTOX green, a bright, low photo-damage DNA intercalating agent, Eur. Biophys. J. 44 (2015) 337–348, http://dx.doi.org/10.1007/s00249-015-1027-8.
[40] B.L. Roth, M. Poot, S.T. Yue, P.J. Millard, Bacterial viability and antibiotic susceptibility testing with SYTOX green nucleic acid stain, Bact. Viability Antibiotic Susceptibility Test. SYTOX Green Nucleic Acid Stain 63 (1997) 2421–2431.
[41] L.H. Armbrecht, V. Smetacek, P. Assmy, C. Klaas, Cell death and aggregate formation in the giant diatom Coscinodiscus wailesii (Gran & Angst, 1931), J. Exp. Mar. Bio Ecol. 452 (2014) 31–39, http://dx.doi.org/10.1016/j.jembe.2013.12.004.
[42] L. Zhang, C. Lei, J. Chen, K. Yang, L. Zhu, D. Lin, Effect of natural and synthetic surface coatings on the toxicity of multiwalled carbon nanotubes toward green algae, Carbon N. Y. 83 (2015) 198–207, http://dx.doi.org/10.1016/j.carbon.2014.11.050.
[43] S.L. Erlandsen, C.J. Kristich, G.M. Dunny, C.L. Wells, High-resolution visualization of the microbial glycocalyx with low-voltage scanning electron microscopy: dependence on cationic dyes, J. Histochem. Cytochem. 52 (2004) 1427–1435, http://dx.doi.org/10.1369/jhc.4A6428.2004.
[44] M. Mathieu, J. Leflaive, L. Ten-Hage, R. De Wit, E. Buffan-Dubau, Free-living nematodes affect oxygen turnover of artificial diatom biofilms, Aquat. Microb. Ecol. 49 (2007) 281–291, http://dx.doi.org/10.3354/ame01150.
[45] R.S. Macedo, A.T. Lombardi, C.Y. Omachi, L.R. Rörig, Effects of the herbicide bentazon on growth and photosystem II maximum quantum yield of the marine diatom Skeletonema costatum, Toxicol. Vitr. 22 (2008) 716–722, http://dx.doi.org/10.1016/j.tiv.2007.11.012.
[46] K. Yang, Y. Li, X. Tan, R. Peng, Z. Liu, Behavior and Toxicity of Graphene and its Functionalized Derivatives in Biological Systems, 2013, pp. 1492–1503, http://dx.doi.org/10.1002/smll.201201417.
[47] S. Kang, M. Herzberg, D.F. Rodrigues, M. Elimelech, Antibacterial effects of carbon nanotubes: size does matter!, Langmuir 24 (2008) 6409–6413, http://dx.doi.org/10.1021/la800951v.
[48] A. Simon-Deckers, S. Loo, M. Mayne-L'hermite, N. Herlin-Boime, N. Menguy, C. Reynaud, et al., Size-, composition-and shape-dependent toxicological impact of metal oxide nanoparticles and carbon nanotubes toward bacteria, Env. Sci. Technol. 43 (2009) 8423–8429, http://dx.doi.org/10.1021/es9016975.
[49] H.L. Karlsson, P. Cronholm, J. Gustafsson, L. Möller, Copper oxide nanoparticles are highly toxic: a comparison between metal oxide nanoparticles and carbon nanotubes, Chem. Res. Toxicol. 21 (2008) 1726–1732, http://dx.doi.org/10.1021/tx800064j.
[50] N. von Moos, V.I. Slaveykova, Oxidative stress induced by inorganic nanoparticles in bacteria and aquatic microalgae-state of the art and knowledge gaps, Nanotoxicology 8 (2013) 1–26, http://dx.doi.org/10.3109/17435390.2013.809810.
[51] A.A. Shvedova, A. Pietriusti, F. Bengt, V.E. Kagan, Mech. carbon nanotube-induced Toxic. Focus oxidative stress 261 (2012) 121–133, http://dx.doi.org/10.1038/nbt.3121.ChIP-nexus.
[52] N. Li, T. Xia, A. Nel, The role of oxidative stress in ambient particulate matter-induced lung diseases and its implications in the toxicity of engineered nanoparticles, Free Radic. Biol. Med. 44 (2008) 1689–1699, http://dx.doi.org/10.1016/j.freeradbiomed.2008.01.028.The.
[53] J.-P. Tessonnier, D.S. Su, Recent progress on the growth mechanism of carbon nanotubes: a review, ChemSusChem 4 (2011) 824–847, http://dx.doi.org/10.1002/cssc.201100175.
[54] L. Guo, A. Von Dem Bussche, M. Buechner, A. Yan, A.B. Kane, R. Hurt, Adsorption of essential micronutrients by carbon nanotubes and the implications for nanotoxicity testing, NIH 4 (2012) 721–727, http://dx.doi.org/10.1016/j.pestbp.2011.02.012.Investigations.
[55] J.F.C. de Brouwer, K. Wolfstein, G.K. Ruddy, T.E.R. Jones, L.J. Stal, Biogenic stabilization of intertidal sediments: the importance of extracellular polymeric substances produced by benthic diatoms, Microb. Ecol. 49 (2005) 501–512, http://dx.doi.org/10.1007/s00248-004-0020-z.
[56] H.C. Flemming, J. Wingender, Relevance of microbial extracellular polymeric substances (EPSs)–Part I: structural and ecological aspects, Water sci. technol. J. Int. asso.c water pollut. res. 43 (2001) 1–8.
[57] Z. Long, J. Ji, K. Yang, D. Lin, F. Wu, Systematic and quantitative investigation of the mechanism of carbon nanotubes' toxicity toward algae, Environ. Sci. Technol. 46 (2012) 8458–8466, http://dx.doi.org/10.1021/es301802g.

[58] F. Schwab, T.D. Bucheli, L.P. Lukhele, A. Magrez, B. Nowack, L. Sigg, et al., Are Carbon Nanotube Effects on Green Algae Caused by Shading and Agglomeration?, 2011, pp. 6136–6144, http://dx.doi.org/10.1021/es200506b.
[59] H.D. Nielsen, L.S. Berry, V. Stone, T.R. Burridge, T.F. Fernandes, Interactions between carbon black nanoparticles and the brown algae Fucus serratus: inhibition of fertilization and zygotic development, Nanotoxicology 2 (2008) 88–97.
[60] K. van Hoecke, J.T.K. Quik, J. Mankiewicz-Boczek, K. a C. De Schamphelaere, A. Elsaesser, P. van Der Meeren, et al., Fate and effects of CeO nanoparticles in aquatic ecotoxicity tests fate and effects of CeO 2 nanoparticles in aquatic ecotoxicity tests, Environ. Sci. Technol. 43 (2009) 4537–4546, http://dx.doi.org/10.1021/es9002444.
[61] V. Aruoja, H.C. Dubourguier, K. Kasemets, A. Kahru, Toxicity of nanoparticles of CuO, ZnO and TiO2 to microalgae pseudokirchneriella subcapitata, Sci. Total Environ. 407 (2009) 1461–1468, http://dx.doi.org/10.1016/j.scitotenv.2008.10.053.
[62] S. Tsunekawa, T. Fukuda, A. Kasuya, Blue shift in ultraviolet absorption spectra of monodisperse CeO[sub 2−x] nanoparticles, J. Appl. Phys. 87 (2000) 1318–1321, http://dx.doi.org/10.1063/1.372016.
[63] K. Hund-rinke, M. Simon, Ecotoxic effect of photocatalytic active nanoparticles (TiO 2) on algae and daphnids, Env. Sci. Pollut. Res. 2006 (2006) 1–8.
[64] J. Ji, Z. Long, D. Lin, Toxicity of oxide nanoparticles to the green algae Chlorella sp, Chem. Eng. J. 170 (2011) 525–530, http://dx.doi.org/10.1016/j.cej.2010.11.026.
[65] Y.-H. Tsuang, J.-S. Sun, Y.-C. Huang, C.-H. Lu, W.H.-S. Chang, C.-C. Wang, Studies of photokilling of bacteria using titanium dioxide nanoparticles, Artif. Organs 32 (2008) 167–174, http://dx.doi.org/10.1111/j.1525-1594.2007.00530.x.
[66] A. Bour, F. Mouchet, J. Silvestre, L. Gauthier, E. Pinelli, Environmentally relevant approaches to assess nanoparticles ecotoxicity: a review, J. Hazard Mater 283 (2015) 764–777, http://dx.doi.org/10.1016/j.jhazmat.2014.10.021.
[67] E. Navarro, A. Baun, R. Behra, N.B. Hartmann, J. Filser, A.-J. Miao, et al., Environmental behavior and ecotoxicity of engineered nanoparticles to algae, plants, and fungi, Ecotoxicology 17 (2008) 372–386, http://dx.doi.org/10.1007/s10646-008-0214-0.
[68] R. Raliya, J.C. Tarafdar, ZnO nanoparticle biosynthesis and its effect on phosphorous-mobilizing enzyme secretion and gum contents in clusterbean (cyamopsis tetragonoloba L.), Agric. Res. 2 (2013) 48–57, http://dx.doi.org/10.1007/s40003-012-0049-z.
[69] G. Hofmann, in: Gabriele Hofmann, Horst Lange-Bertalot, Marcus Werum (Eds.), Diatomeen im Süßwasser-Benthos von Mitteleuropa: Bestimmungsflora Kieselalgen für die ökologische Praxis: über 700 der häufigsten Arten und ihre Ökologie/Horst Lange-Bertalot, Königstein: Koeltz Scientific Books, 2013.
[70] A. Miao, K.A. Schwehr, C. Xu, S. Zhang, Z. Luo, A. Quigg, et al., The algal toxicity of silver engineered nanoparticles and detoxification by exopolymeric substances, Environ. Pollut. 157 (2009) 3034–3041, http://dx.doi.org/10.1016/j.envpol.2009.05.047.
[71] N. Joshi, B.T. Ngwenya, C.E. French, Enhanced resistance to nanoparticle toxicity is conferred by overproduction of extracellular polymeric substances, J. Hazard Mater 241–242 (2012) 363–370, http://dx.doi.org/10.1016/j.jhazmat.2012.09.057.
[72] T.A. Davis, B. Volesky, A. Mucci, A review of the biochemistry of heavy metal biosorption by brown algae, Water Res. 37 (2003) 4311–4330, http://dx.doi.org/10.1016/S0043-1354(03)00293-8.
[73] L. Verneuil, J. Silvestre, I. Randrianjatovo, C.-E. Maracato-romain, E. Girbal-Neuhauser, F. Mouchet, et al., Double walled carbon nanotubes promote the overproduction of extracellular protein-like polymers in Nitzschia palea : an adhesive response for an adaptive issue, Carbon N. Y. (2015) 88, http://dx.doi.org/10.1016/j.carbon.2015.02.053.
[74] J. Wang, K.W. Bayles, Programmed cell death in plants: lessons from bacteria? Trends Plant Sci. 18 (2013) 133–139, http://dx.doi.org/10.1016/j.tplants.2012.09.004.
[75] L. Tang, A. Schramm, T.R. Neu, N.P. Revsbech, R.L. Meyer, Extracellular DNA in adhesion and biofilm formation of four environmental isolates: a quantitative study, FEMS Microbiol. Ecol. 86 (2013) 394–403, http://dx.doi.org/10.1111/1574-6941.12168.